Article

Retrograde GABA Signaling Adjusts Sound Localization by Balancing Excitation and Inhibition in the Brainstem

Anna K. Magnusson,[1,*] Thomas J. Park,[2] Michael Pecka,[1,3] Benedikt Grothe,[1,3,4] and Ursula Koch[1,4,*]

[1]Department Biologie II, Division of Neurobiology, LMU Munich, Grosshadernerstrasse 2, 82152 Martinsried, Germany
[2]Department of Biological Sciences, Neurobiology Group, University of Illinois, Chicago, IL 60607, USA
[3]Bernstein Center for Computational Neuroscience, 81377 Munich, Germany
[4]These authors contributed equally to this work
*Correspondence: anna.magnusson@ki.se (A.K.M.), koch@zi.biologie.uni-muenchen.de (U.K.)
DOI 10.1016/j.neuron.2008.05.011

SUMMARY

Central processing of acoustic cues is critically dependent on the balance between excitation and inhibition. This balance is particularly important for auditory neurons in the lateral superior olive, because these compare excitatory inputs from one ear and inhibitory inputs from the other ear to compute sound source location. By applying GABA_B receptor antagonists during sound stimulation in vivo, it was revealed that these neurons adjust their binaural sensitivity through GABA_B receptors. Using an in vitro approach, we then demonstrate that these neurons release GABA during spiking activity. Consequently, GABA differentially regulates transmitter release from the excitatory and inhibitory terminals via feedback to presynaptic GABA_B receptors. Modulation of the synaptic input strength, by putative retrograde release of neurotransmitter, may enable these auditory neurons to rapidly adjust the balance between excitation and inhibition, and thus their binaural sensitivity, which could play an important role as an adaptation to various listening situations.

INTRODUCTION

An appropriate balance between excitation and inhibition is essential for functional sensory networks. For example, the relative strength and timing of excitatory and inhibitory inputs shapes the response to sensory stimuli, which is critical for the organization and tuning of receptive fields (Wehr and Zador, 2003; Zhang et al., 2003; Marino et al., 2005; Higley and Contreras, 2006). Dynamic adjustment of the balance between excitation and inhibition is especially important for auditory neurons that rely on precise comparison of excitatory and inhibitory inputs, such as the neurons of the lateral superior olive (LSO). The LSO is an auditory brainstem nucleus that encodes interaural sound level differences (ILDs), which is one of the main cues used for sound localization (Finlayson and Caspary, 1989; Park et al., 1996). Analysis of ILDs is accomplished by a direct subtraction of an in-

hibitory, glycinergic input, activated by sound arriving at the contralateral ear, from an excitatory input, activated by sound arriving at the ipsilateral ear (Boudreau and Tsuchitani, 1968; Moore and Caspary, 1983; Finlayson and Caspary, 1989). A key question is how this neuronal circuit adjusts the balance between excitation and inhibition to adapt to changes in the sensory environment. On a cellular level, adjustments to the synaptic strength of the inputs, or the integrative properties of the neurons, could control the complex interplay between excitation and inhibition. One possible candidate for this task is GABA_B receptors, which are present presynaptically on the inputs to LSO neurons (Kotak et al., 2001). Such G protein-coupled receptors are able to modulate both synaptic inputs and postsynaptic properties (reviewed by Miller, 1998), and could therefore be important for the fine-tuning of sensory networks. In the present study, we tested the hypothesis that LSO neurons adjust their ILD sensitivity by regulating the balance of their excitatory and inhibitory inputs via GABA_B receptors. By using a combined in vivo and in vitro approach, we show that the LSO neurons release GABA, which acts as a retrograde transmitter on presynaptic GABA_B receptors. Furthermore, activation of the presynaptic GABA_B receptors differentially controls the excitatory and inhibitory terminals in the LSO. This results in a shift of the dynamic range of the ILD function (i.e., the ILD sensitivity), thus narrowing the binaural receptive field of the neurons. We propose that by adjusting the balance between excitation and inhibition, LSO neurons can rapidly adapt their binaural response properties and thereby accommodate the current acoustic environment.

RESULTS

GABA_B Receptors Modulate the Sensitivity of LSO Neurons to Sound Level Differences between the Ears

The spike response of single LSO neurons to sounds with various ILDs, presented via earphones, was recorded in adult anaesthetized gerbils. The LSO neurons responded strongly to sound stimulation that favored the ipsilateral ear (positive ILDs) and were progressively inhibited by increasing the sound level at the contralateral ear (negative ILDs) (Figure 1A, left panel). To examine the role of GABA_B receptor activation on ILD processing, the GABA_B receptor agonist baclofen and the antagonists CGP35348 and CGP55845 were applied iontophoretically while
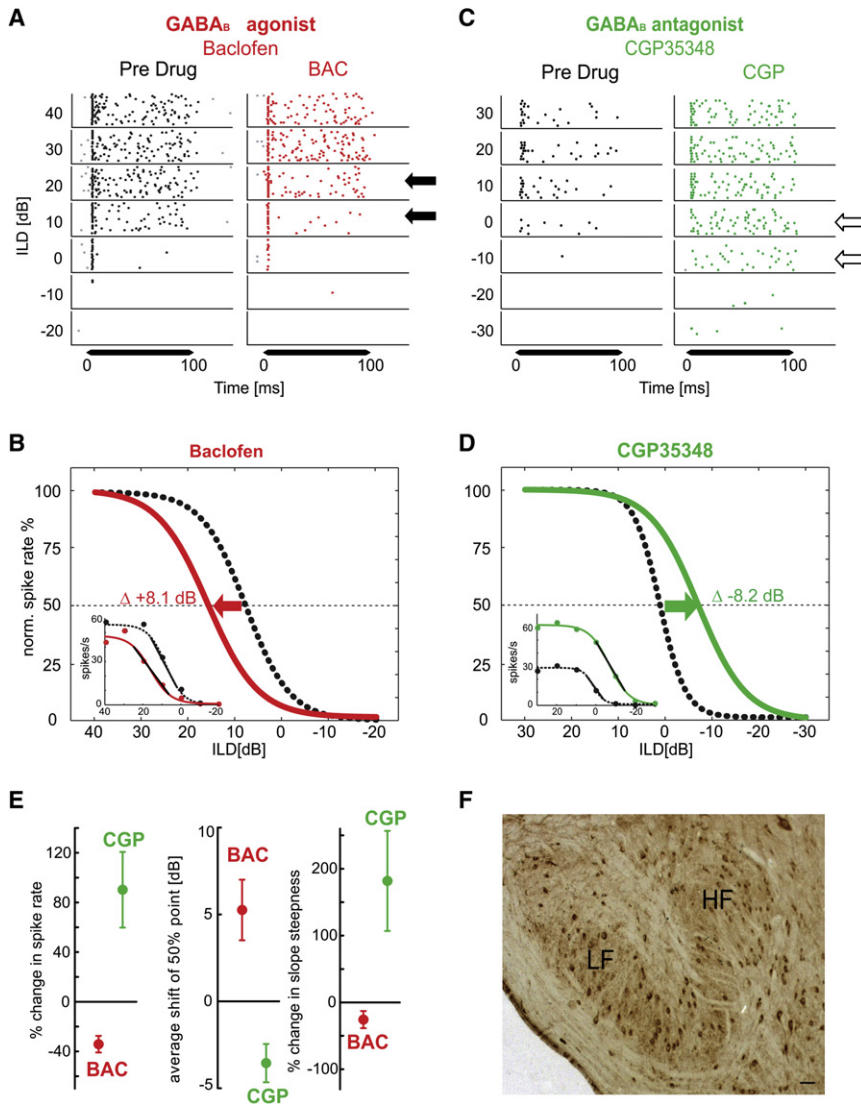
Figure 1. Pharmacological Manipulation of GABA_B Receptors In Vivo Causes a Shift in Neuronal Sensitivity to Interaural Sound Level Difference, an Important Cue Used for Sound Localization

(A) Dot raster plots of one example neuron for various interaural sound level differences (ILDs) before (left panel) and during (right panel) iontophoretic application of the GABA_B receptor agonist baclofen. Each dot corresponds to one action potential. Sound stimuli consisted of 100 ms pure tones presented at the neuron's best response frequency. The amplitude at the excitatory, ipsilateral ear was set 20 dB above response threshold and each ILD was presented 20 times in pseudorandom order. Sounds that were more intense at the contralateral, inhibitory ear (negative ILDs) generated fewer action potentials in the predrug condition; baclofen increased this spike suppression (e.g., at ILDs of 10 and 20 dB, arrows).

(B) Normalized fitted ILD functions corresponding to the dot raster plots in (A) (dashed black line = predrug; solid red = baclofen). The ILD at 50% of normalized peak response was used as an index of drug-induced effects. This neuron showed an 8.1 dB shift in the 50% point ILD during baclofen application (50% suppression was achieved with tones that were 8.1 dB less intense at the contralateral, inhibitory ear than what was required without baclofen). The inset shows nonnormalized ILD functions.

(C) Dot raster plots from a different neuron recorded before and during application of the GABA_B receptor antagonist CGP35348 (5 mM). The antagonist caused a robust increase in spikes at ILDs of 0 and −10 dB (open arrows), the opposite effect to that of baclofen.

(D) Normalized ILD functions corresponding to the dot raster plots in (C). Application of the antagonist caused an 8.2 dB shift in the 50% point toward negative ILD values.

(E) (Left panel) Mean change in spike rate (±SEM) induced by application of baclofen (red, n = 13) or the antagonists CGP35348 and CGP55845 (green, n = 19 and 3, respectively; data from the two antagonists was pooled since there was no statistical difference between the results). (Middle panel) Mean shift in 50% point ILDs (±SEM) due to the agonist baclofen and due to the antagonists CGP35348 and CGP55845. The latency from initiation of drug iontophoresis to the onset of the effect was between 140 and 200 s. (Right panel) Mean change in slope of the unnormalized ILD function induced by GABA_B receptor activation or inactivation.

(F) GABA_B receptor immunoreactivity in the adult gerbil LSO. Immunostained neurons are evident in the high-frequency (HF) and low-frequency (LF) region of the LSO. Scale bar: 50 μm.

recording the spike response to sounds with various ILDs. For further analysis the spike response was fitted with a sigmoid function. Baclofen (50 mM; n = 13) generally decreased the maximal discharge rate evoked by sounds favoring the ipsilateral, excitatory ear by 34.2% ± 6.7% (Figure 1E). Importantly, activation of GABA_B receptors also resulted in a suppression of the ILD response such that more suppression was exerted at more positive ILDs (Figure 1A, right panel, closed arrows). This relative decrease in spike number, induced by GABA_B receptor activation, resulted in a systematic shift of the normalized ILD function toward more positive ILDs, thereby narrowing the binaural response area of the neuron toward ILDs that correspond to more ipsilateral sound positions (Figure 1B). Conversely, ionto-

phoretic application of the GABA_B receptor antagonist CGP35348 (100 mM; n = 19) or CGP55845 (5 mM; n = 3) resulted in the opposite effect (Figures 1C and 1D). Spike numbers for sounds favoring the ipsilateral, excitatory ear increased by 90.2% ± 30.5% (Figure 1E). As during GABA_B receptor activation, this increase in spike count was dependent on the spike rate during ILD presentation. GABA_B receptor blockade caused a substantial spike response at ILDs where only a weak spike response had been observed under control conditions (Figure 1C, open arrows). This resulted in a shift of the normalized ILD functions toward more negative ILDs, thus expanding the binaural response area of the neurons to include ILDs that correspond to more contralateral sound source locations (Figure 1D). This

negative shift of the ILD function also confirms the specificity of the opposite ILD shift during $GABA_B$ receptor activation. For all neurons tested, the ILD shift measured at the ILD where the spike response had decreased to 50% of the maximum response was 5.3 ± 1.7 dB ($p \leq 0.001$; n = 22) toward positive ILDs during $GABA_B$ receptor activation and 3.6 ± 1.1 dB ($p \leq 0.001$; n = 13) toward negative ILDs during $GABA_B$ receptor blockade (Figure 1E). Neurons with binaural response areas extending more towards contralateral sound locations (negative ILDs) were more affected by baclofen than neurons with binaural response areas closer to the ipsilateral side (positive ILDs) (Figure S1, available online). To assess whether $GABA_B$ receptor activation or inactivation resulted in a gain change of the ILD response, the steepness of the sigmoid function was analyzed (Figures 1B and 1D, insets). On average, the slope of the ILD function increased by $181.8\% \pm 74.9\%$ ($p \leq 0.05$; n = 22) during $GABA_B$ receptor blockade, whereas $GABA_B$ receptor activation had the opposite effect on the slope (Figure 1E), indicating that $GABA_B$ receptors exert a divisive (multiplicative) gain control function on the ILD coding of LSO neurons.

Since there is no morphological evidence for $GABA_B$ receptors in the gerbil LSO in the literature, a conventional antibody staining was performed in order to demonstrate the presence of the receptors. It confirmed that $GABA_B$ receptors are abundant on LSO neurons throughout the nucleus (Figure 1F) but could not determine the subcellular location of the receptor.

Taken together, these data demonstrate that endogenous $GABA_B$ receptor activation in the LSO systematically influences the ILD sensitivity by modulating the binaural response properties of the LSO neurons. Moreover, $GABA_B$ receptor activation in the LSO also scales the spike rates in a divisive manner, which is compatible with the concept of neural gain control. On an operational level, the ILD sensitivity of LSO neurons is determined by comparing the excitatory and inhibitory inputs from the two ears. Hence, the opposite shifts of the ILD function during $GABA_B$ receptor activation and inactivation suggest that the excitatory inputs from the ipsilateral ear and the inhibitory inputs from the contralateral ear are differentially controlled by $GABA_B$ receptors.

The ILD Shift Is Mediated by Presynaptic $GABA_B$ Receptors in the LSO

Mechanistically, the modulation of LSO neurons described above could occur through activation of presynaptic $GABA_B$ receptors on the excitatory or the inhibitory terminals, where they control transmitter release. Alternatively, modulation may be due to activation of postsynaptic $GABA_B$ receptors, which might modulate the integration of these inputs to the LSO (reviewed by Nicoll, 2004). To address this issue, we made whole-cell voltage-clamp recordings from putative LSO principal neurons, selected according to their physiological properties (Figure S2A), in acute brainstem slices of post-hearing-onset gerbils.

Presynaptic $GABA_B$ receptors at the LSO synapses were investigated by recording either pharmacologically isolated excitatory postsynaptic currents (EPSCs), evoked by stimulating the cochlear nucleus fibers from the ipsilateral ear, or inhibitory postsynaptic currents (IPSCs), evoked by stimulating the trapezoid fiber bundle (input from the contralateral ear) (Figure 2A). Cesium

was included in the pipette to block $GABA_B$ receptor-activated K^+ channels. Bath application of baclofen (1 μM), a $GABA_B$ receptor agonist, reversibly reduced the amplitude of evoked AMPA and NMDA receptor-mediated EPSCs as well as glycinergic IPSCs (Figure 2B). To verify that the reduction in amplitude was caused exclusively by $GABA_B$ receptors, we repeated the same experiment in the presence of specific $GABA_B$ receptor antagonists (CGP55845, 3 μM or SCH50911, 10 μM). Bath application of the $GABA_B$ receptor antagonists blocked the baclofen-induced reduction of the EPSCs and the IPSCs (Figure 2D), confirming that the effects of the agonist are mediated by stimulation of $GABA_B$ receptors. The fact that the $GABA_B$ receptor antagonists had no effect per se (Figure 2D) suggests that there is no tonic activation of the $GABA_B$ receptors by ambient GABA in the slice. The dose-response relationship of baclofen-mediated inhibition revealed a significantly more potent activation of $GABA_B$ receptors at the excitatory synapses (half-maximal inhibitory concentration $[IC_{50}] = 0.56$ μM) than at the inhibitory synapses ($IC_{50} = 1.52$ μM) (Figure 2C), which is in line with our in vivo finding that $GABA_B$ receptor blockade favors excitation rather than inhibition (Figure 1). Furthermore, baclofen (10 μM) increased the paired-pulse ratio (PPR), a measure of the probability of transmitter release, of the EPSCs (control, 0.83 ± 0.04; baclofen, 1.38 ± 0.36; $p < 0.05$, n = 6) and IPSCs (control, 0.78 ± 0.04; baclofen, 0.93 ± 0.03; $p < 0.01$, n = 5), providing evidence for a presynaptic mechanism of action.

To determine whether activation of postsynaptic $GABA_B$ receptors elicits a response in these neurons, we applied exogenous baclofen (10 μM) by puffing the agonist directly onto the neuron (n = 10). Application of baclofen would be expected to generate an outward current recorded at -60 mV with a K^+-based intracellular solution, but we could not observe such a response (Figure 2E). To make sure that the lack of response was not related to some technical issue, we puffed baclofen from the same pipette onto medial vestibular neurons (n = 3), known to have postsynaptic $GABA_B$ receptors (Dutia et al., 1992; Holstein et al., 1992), in the same slice. Under voltage clamp, baclofen triggered a long-lasting outward current, and under current clamp, baclofen induced a membrane hyperpolarization accompanied by a cessation of spontaneous action potential discharges (data not shown). To exclude that GABA could exert a postsynaptic effect on the intrinsic excitability of the LSO neurons via $GABA_B$ receptors, spike trains were elicited by injecting 50 Hz trains of excitatory postsynaptic conductances (EPSGs) into the cells before and during baclofen (3 μM) application. There was no qualitative change in the neurons' spiking activity during bath application of baclofen (3 μM) (Figure 2G), and a quantification of spike threshold (control, -43 ± 2 mV; baclofen, -43 ± 2 mV), spike amplitude (control, 67 ± 3 mV; baclofen, 66 ± 4 mV), and spike width (control, 0.51 ± 0.04 ms; baclofen, 0.51 ± 0.05 ms) did not reveal any further effects of $GABA_B$ receptor activation in these cells (n = 5). The fact that input resistance did not change upon application of baclofen in the LSO (control, 51 ± 16 MΩ; baclofen, 52 ± 16 MΩ; $p = 0.58$, n = 10) lends further support to a presynaptic mechanism of action. We therefore conclude that, in the LSO, postsynaptic $GABA_B$ receptors do not modulate postsynaptic voltage-dependent ion conductances, such as K^+ and Ca^{2+} currents, or have immediate effects on the intrinsic excitability. However, postsynaptic $GABA_B$
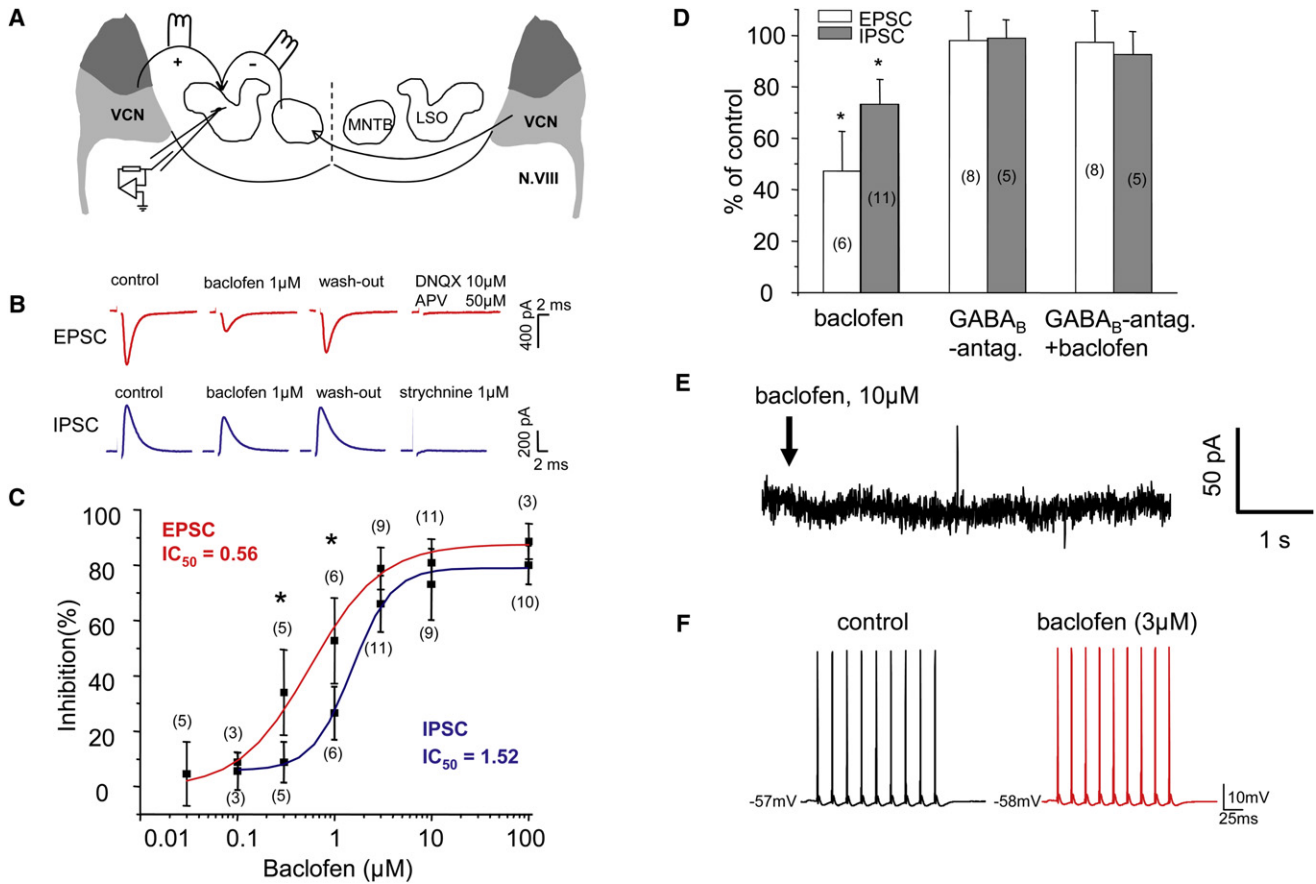
Figure 2. Baclofen Inhibits Synaptic Transmission in the LSO

(A) Schematic overview of the preparation, which consists of transverse brainstem slices containing the LSO and its auditory nerve input (N. VIII). The excitatory fibers from the ventral cochlear nucleus (VCN) and the inhibitory fibers from the medial nucleus of the trapezoid body (MNTB) are stimulated with a glass microelectrode filled with 2 M NaCl.

(B) Bath application of baclofen (1 μM) reversibly inhibited glutamatergic (red) and glycinergic (blue) postsynaptic currents; each response represents an average of 20 traces.

(C) Concentration dependency and IC_{50} of baclofen-mediated inhibition of the EPSCs and IPSCs.

(D) A prior application of a $GABA_B$ receptor antagonist (10 μM SCH50911 or 3 μM CGP55845) had no effect on the amplitude of the synaptic inputs and blocked the inhibition of baclofen (1 μM).

(E) Pressure application (20 psi, 0.1 s) of baclofen (10 μM) in the LSO (upper trace). Baclofen did not elicit any current flow across the membrane in the LSO.

(F) Spike response evoked by postsynaptic injection of high-frequency EPSGs via a conductance-clamp amplifier under control conditions and during baclofen application (3 μM). No change in spike amplitude and spike shape was observed during $GABA_B$ receptor activation as compared to control conditions. *$p < 0.05$. For (D) and (E), the number of cells recorded for each concentration is given in parenthesis.

receptors could be involved in long-term plastic changes, as shown before hearing onset (Kotak et al., 2001; Chang et al., 2003).

GABA Acts as a Retrograde Transmitter in the LSO

We have shown that GABA exerts a strong influence on LSO neurons through presynaptic $GABA_B$ receptors. A critical question is, "Where does the GABA come from?"

Many of the LSO neurons are GABAergic (Roberts and Ribak, 1987; Helfert et al., 1989; Gonzalez-Hernandez et al., 1996), and one possible scenario is that the LSO neurons themselves release GABA, which affects their synaptic inputs in an autocrine or paracrine fashion (reviewed by Ludwig and Pittman, 2003; Zilberter et al., 2005). We evaluated this hypothesis by investi-

gating what effect depolarization of the LSO neurons had on pharmacologically isolated excitatory postsynaptic potentials (EPSPs). After several minutes of stable EPSP responses (control), the synaptically evoked potentials were paired with a preceding 100–200 Hz train of action potentials (conditioning), which was induced by somatic current injections (Figure S2A). Conditioning trains of action potentials rapidly decreased the EPSP amplitude. This effect was reversible and could be induced again after recovery (Figure 3A). There was a significant reduction in EPSP amplitude (control, 4.3 ± 1.9 mV; conditioning, 2.9 ± 1.9 mV; p < 0.001, n = 13), accompanied by an increase in the PPR (control, 0.80 ± 0.12; conditioning, 1.45 ± 0.93; p < 0.001, n = 13), suggesting a decrease in transmitter release in response to the conditioning.

To obviate the contribution of postsynaptic voltage-gated ion channels to these effects, two experimental designs were employed. First, we determined the increase in failure rate in response to conditioning trains when the stimulation of the excitatory inputs was adjusted to just above the threshold for an evoked response with only a few failures (~10% failure rate). Again, after several minutes of stable responses (control), the synaptically evoked potentials were paired with a 100–200 Hz preceding train of action potentials (conditioning). Conditioning rapidly increased the probability of failure of the EPSPs (control, 6.4% ± 8.3%; conditioning, 35.4% ± 17.3%; p < 0.001, n = 13). This effect was dependent on the frequency of the conditioning train (Figure S2B) and the intensity of the somatic current injection (Figure S2C). The increase in failures during conditioning also resulted in a striking reduction of the mean EPSP amplitude in 31 of 43 (or 72% of) LSO neurons and a corresponding increase in the PPRs of EPSPs, in a very similar manner to that of the larger-amplitude EPSPs and the classical baclofen-induced increase in the PPR. A summary of the effects of conditioning on EPSPs is given in Figure 3C. This form of short-term presynaptic depression of the EPSPs was effectively blocked by the three different $GABA_B$ receptor antagonists: CGP35348 (100–200 μM), CGP55854 (3 μM), or SCH50911 (10 μM) (Figures 3B and 3C), which strongly indicates that GABA acts as a retrograde transmitter on presynaptic $GABA_B$ receptors in the LSO. Moreover, the input resistance of the neurons remained stable during the conditioning stimuli (control, 64 ± 22 MΩ; conditioning, 65 ± 23 MΩ; p = 0.83, n = 10), also supporting the concept of a presynaptic mechanism.

In a second approach, EPSCs evoked in the same way as in the current-clamp recordings were measured in voltage-clamp mode under control conditions and with a preceding depolarization of the neuron (duration: 500 ms, to 0 mV). As for the EPSPs, the preceding depolarization caused a significant reduction of the EPSC amplitude (control, 1002 ± 182 pA; depolarization, 797 ± 167 pA; p < 0.001, n = 7) (Figure 3D) and an increase in the PPR (control, 0.75 ± 0.05; depolarization, 0.84 ± 0.05; p < 0.01, n = 7) (Figure 4D). Bath application of $GABA_B$ receptor antagonists to the same neurons prevented the decrease in EPSC amplitude (control, 905 ± 180 pA; depolarization, 868 ± 180 pA; n = 7) and the increase in the PPR (control, 0.8 ± 0.05; depolarization, 0.77 ± 0.05; n = 7), indicating a similar mechanism for the amplitude reduction of the excitatory currents as for the EPSPs following a preceding train of action potentials.

It is, however, essential to know whether the reduced EPSP/EPSC amplitude during conditioning is related to lessened synaptic release of transmitter or due to a failure to activate the axon/synaptic bouton. To elucidate this, the effect of 500 ms depolarizing voltage steps to +30 mV on spontaneous release of transmitter was investigated in voltage-clamped LSO neurons. The frequency of pharmacologically isolated spontaneous EPSCs (sEPSCs) decreased by 21% (control, 3.6 ± 0.7 Hz; depolarization, 2.8 ± 0.64 Hz; p < 0.01, n = 14) (Figure 3E), whereas the amplitude of the sEPSCs remained stable (control, 64 ± 7 pA; depolarization, 63 ± 7 pA). Also, the reduction of sEPSC frequency with depolarizing conditioning was blocked by the $GABA_B$ receptor antagonist SCH50911 (control, 2.6 ± 0.38 Hz;

conditioning, 2.5 ± 0.38 Hz; n = 11) (Figure 3E). These results demonstrate that the most likely reason for the decrease in EPSP amplitude and the increase in failure rate observed during conditioning is a decrease in the release of transmitter from the presynaptic bouton in response to the presynaptic $GABA_B$ receptor activation.

GABA could be released either from the dendrites of the LSO neurons themselves or from axon collaterals projecting back to the cell as autapses. These possibilities were tested by adding either QX314 (a sodium channel blocker), BAPTA (a calcium chelator) or botulinum neurotoxin D light chain (BoNT D) to the intracellular recording solution. Addition of QX314 (5 mM) effectively prevented the cell from firing action potentials within a few minutes. The conditioning trains thus only depolarized the cell and activated their Ca^{2+} channels. Nevertheless, we still observed a decrease in EPSP amplitude accompanied by an increase of the PPR during conditioning stimuli (Figure 4A), which indicates that GABA is most probably not released from back-projecting axon collaterals. In contrast, BAPTA (10 mM) effectively prevented the EPSP amplitude reduction and the PPR increase during conditioning trains of action potentials (Figure 4B), pointing toward a Ca^{2+}-dependent mechanism. BoNT D is known to cleave synaptobrevin, a protein that is part of the plasma membrane SNARE protein complex, which is essential for Ca^{2+}-induced vesicle exocytosis (Schoch et al., 2001). Inclusion of BoNT D (1–2 μg/ml) into the pipette also blocked the effect of conditioning on the EPSP amplitude and the PPR (Figure 4C). Taken together, this is consistent with the hypothesis that GABA is released via exocytosis in a Ca^{2+}-dependent manner from the LSO dendrites (or somas).

If GABA is exocytosed from LSO dendrites, the vesicles should contain vesicular GABA transporter (VGAT). Accordingly, we performed a triple immunostaining against VGAT (red), MAP2 (green),and Nissl (blue), which colabeled the dendrites and somata of LSO neurons (Figures 4D–4F). Based on the knowledge that the major inhibitory input to the LSO is glycinergic (Moore and Caspary, 1983; Sanes et al., 1987), and that VGAT is also identified as a vesicular glycine transporter (Chaudhry et al., 1998), most of the VGAT staining was of presynaptic origin and localized to putative glycinergic terminals (Figure 4D, arrow). However, many LSO neurons displayed a clear colocalization of the VGAT puncta and the MAP2 staining, suggesting presence of VGAT in the dendrites as well (Figures 4D and S3A). This was further confirmed by scrutinizing overlays of the VGAT and MAP2 staining at high magnification and 3D reconstructions, which revealed the presence of VGAT puncta inside the dendrites of LSO principal neurons (Figures 4E and 4F). This finding corroborates a post-embedding immunogold labeling study that demonstrated that the somata of LSO neurons are weakly immunopositive to VGAT in the rat (Chaudhry et al., 1998).

Retrograde GABA Signaling Differentially Controls Excitatory and Inhibitory Transmitter Release in the LSO

Conditioning trains of action potentials also affected glycinergic inhibitory postsynaptic potentials (IPSPs), evoked by stimulation of the fibers of the medial nucleus of the trapezoid body. A postsynaptic 100–200 Hz stimulation induced a reduction of the IPSP
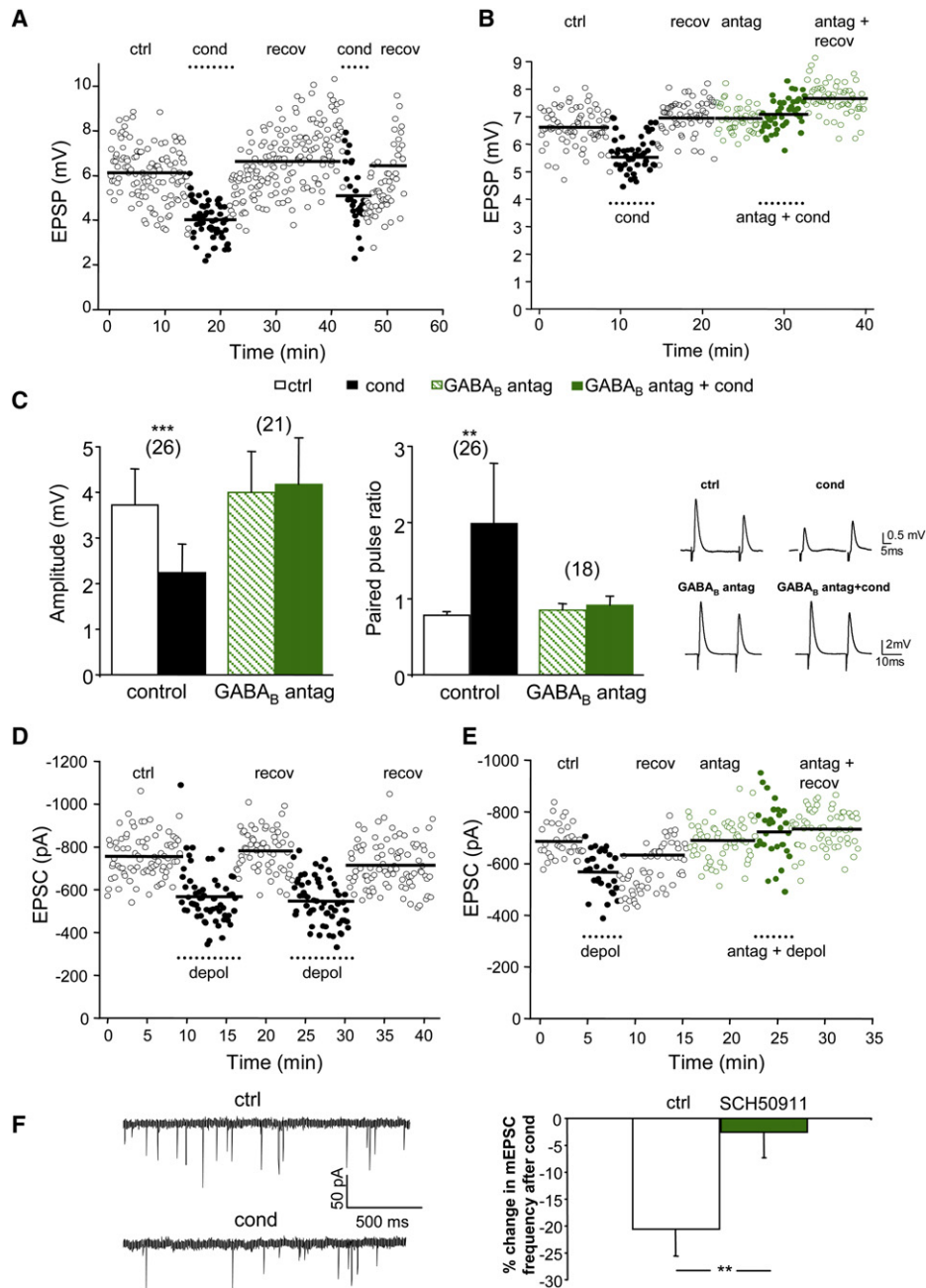
Figure 3. Conditioning Causes a Reversible and GABA$_B$ Receptor-Dependent Depression of the Excitatory Synapses in the LSO

(A) Example EPSPs elicited at ~2 times threshold during control (open circles) and during conditioning (filled circles). The course of the conditioning stimuli is represented by the dotted lines (200 Hz, 1.5 nA). The mean EPSP amplitudes during the respective intervals indicated above the graphs are displayed as horizontal black lines overlaying the dot displays.

(B) The depression of control EPSPs (open circles), achieved by conditioning (filled circles; dotted lines, 200 Hz, 3.5 nA), is blocked by wash-in of a GABA$_B$ receptor antagonist (open green circles, SCH95011, 10 μM) before applying the same conditioning (filled green circles).

(C) Summaries (mean ± confidence interval [c.i.]) of the amplitude and the PPR under control conditions (white bars) following 100–200 Hz conditioning trains (black bars), and with different GABA$_B$ receptor antagonists (CGP35348, 100–200 μM, n = 8; CGP55845, 3–10 μM, n = 11, SCH50911, 10 μM, n = 2) (control: open green bars; conditioning: green bars). The number of cells recorded for each condition is given in parentheses. Representative examples of the average EPSP PPR during control and during 200 Hz conditioning, for the predrug condition and with GABA$_B$ receptor antagonists, are shown to the right of the histograms (averages ≥ 45 responses).

(D) The EPSC amplitude is reversibly suppressed by a 500 ms long preceding depolarization (depol.) of the neuron to 0 mV and can be repeatedly induced. Each dot represents the peak amplitude of a single EPSCs evoked by stimulation of the ipsilateral cochlear nucleus fibers with a repetition rate of 0.14 Hz during control (open circles) and with preceding depolarization (filled circles). The course of the depolarization is represented by dotted
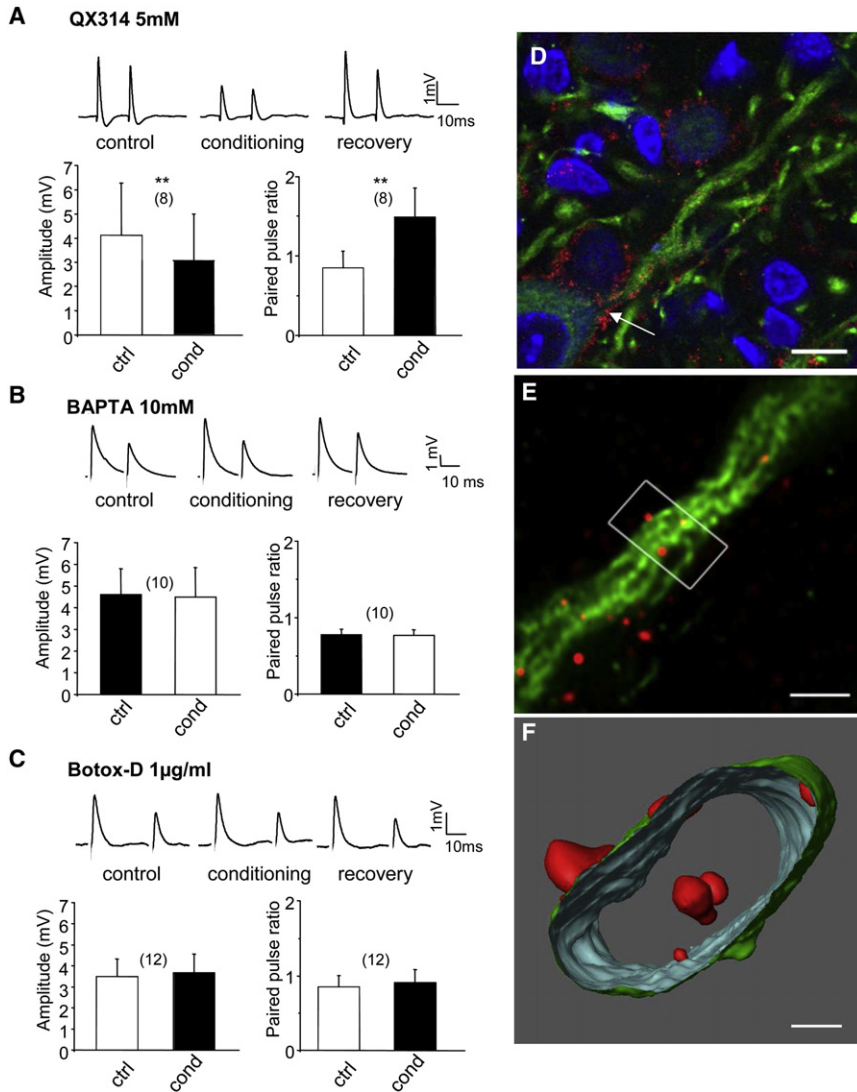
Figure 4. The Increase in Synaptic Failures by Conditioning Is Related to Vesicular Release of GABA

(A–C) Depression of the EPSP amplitudes and increase in PPRs at an interstimulus interval of 30 ms (averages of ≥ 50 responses) in conjunction with 200 Hz conditioning trains (averages of ≥ 50 responses) is not prevented by intracellular loading of the Na^+ channel antagonist QX314 (5 mM) (A), but is effectively prevented by intracellular loading of the Ca^{2+} chelator BAPTA (10 mM) (B) or BoNT D (1–2 $\mu g/ml$) (C). Summaries (mean ± c.i.) of the EPSP amplitudes and the PPRs before (unfilled columns) and after (black columns) conditioning trains are displayed for the three drugs used. The number of cells recorded for each condition is given in parentheses. **p < 0.01.

(D) Laser-scanning microscopy of the vesicular GABA transporter (VGAT, red), MAP2 (green), and Nissl Deep Red (blue) triple labeling in an LSO principal neuron. Arrow indicates VGAT-immunoreactive synaptic terminals with presumed MNTB origin on an LSO principal neuron.

(E) High-magnification image of the same LSO principal neuron revealed significant dendritic VGAT-like immunoreactivity.

(F) The dendritic location of VGAT was confirmed by applying the Huygens (SVI) maximum-likelihood-estimation deconvolution algorithm followed by 3D reconstructions (Amira 3.1, TGS). Surface rendering was applied for the MAP2 staining to highlight the borders of the dendrites.

Axial distance between optical sections: (D) 0.3 μm; (E) and (F) 0.1 μm. Scale bars: (D) 10 μm, (E) 1 μm, (F) 0.5 μm.

tude (EPSPs: 40.3% ± 8.8%, n = 26; IPSPs: 20.6% ± 20.3%, n = 21; p < 0.01), as well as the increase of the PPR (EPSPs: 109.7% ± 61.9%, n = 26; IPSPs: 31.1% ± 24.2%, n = 10; p < 0.05), was

amplitude (control, 4.4 ± 2.3 mV; conditioning, 3.5 ± 2.0 mV; p < 0.001, n = 21), which was paralleled by an increase in the PPR (control, 0.86 ± 0.10; conditioning, 1.15 ± 0.25; p < 0.01, n = 10), in 26 of 74 (or 35% of) LSO neurons tested (Figures 5A and 5C). Similar to the evoked excitation, this effect could be effectively blocked by addition of GABA_B receptor antagonists to the bath (Figures 5B and 5C). A quantitative comparison of the effect of conditioning between EPSPs and IPSPs revealed several differences (Figure 5D). First, the total number of neurons in which this effect was triggered was more than twice as large for EPSPs as it was for IPSPs. Second, the reduction in ampli-

significantly larger for EPSPs than it was for IPSPs (Figure 5D). These results indicate that, during ongoing stimulation, activation of presynaptic GABA_B receptors shifts the balance between the inputs to the LSO by attenuating the excitation relative to the inhibition, which is compatible with our in vivo findings.

An important question that remains is, "What mechanism underlies these differential effects on the excitatory and the inhibitory inputs to the LSO?" It is well known that presynaptically located GABA_B receptors modulate neurotransmitter release (reviewed by Miller, 1998). Since changes in the frequency of miniature events are generally thought to reflect modulation of the

lines, and the mean EPSC amplitudes during the respective intervals indicated above the graphs are displayed as horizontal black bars overlaying the dot displays.

(E) Example in which the GABA_B receptor antagonist SCH50911 (10 μM) was bath-applied 8 min (open green circles) before the second phase of preceding depolarizing pulses (filled green circles). The depolarization-induced suppression of the EPSC amplitude was effectively prevented by the GABA_B receptor blockade.

(F) Individual traces demonstrating that conditioning (500 ms long depolarizing pulses to 30 mV) decreases the frequency of spontaneous EPSCs (sEPSCs), isolated with strychnine (0.5 μM). The decrease in sEPSC frequency (n = 14) is blocked by the GABA_B receptor antagonist SCH50911 (10 μM, n = 11). **p < 0.01; ***p < 0.001.
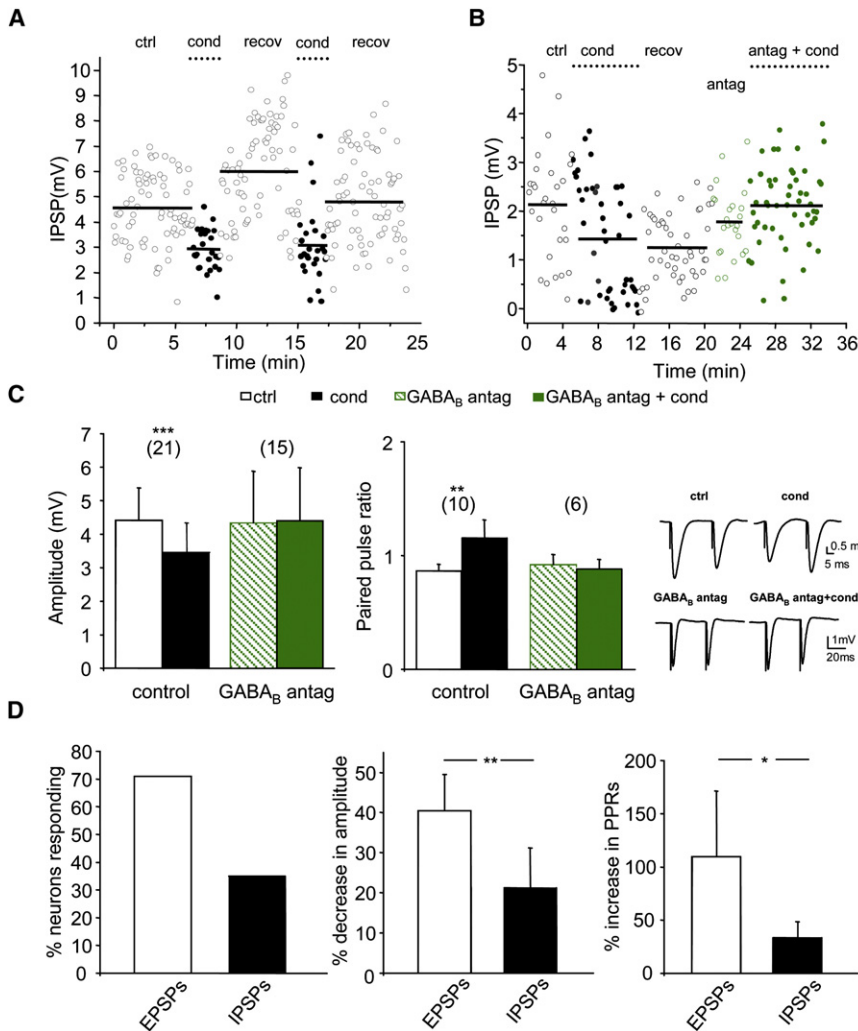
Figure 5. The Effect of Conditioning on Inhibitory Synapses in the LSO Is Smaller Than the Effect on Excitatory Synapses

(A) IPSP amplitudes during control (open circles) and conditioning trains of action potentials (filled circles; 100 Hz, 3 nA) or (B) during control and conditioning (100 Hz, 1 nA) followed by administration of a GABA$_B$ receptor antagonist (open green circles) with the same conditioning (filled green circles). The course of the conditioning stimuli is represented by the dotted lines. The mean IPSP amplitudes during the respective intervals indicated above the graphs are displayed as horizontal black lines overlaying the dot displays. (C) Summaries (mean ± c.i.) of the decrease in amplitude and the increase in the PPR with conditioning trains are illustrated in the histograms. The GABA$_B$ receptor antagonists CGP55845 (3 μM; n = 4 or n = 1, respectively) and SCH50911 (10 μM; n = 11 or n = 5, respectively) were used. Representative examples of the average IPSP PPRs during control and during 100 Hz conditioning are shown to the right of the histograms (average of ≥50 responses). (D) Quantification and comparison of the effects of conditioning trains of action potentials on EPSPs and IPSPs (mean ± c.i.). The excitatory synaptic input to the LSO is more affected by the conditioning. *p < 0.05; **p < 0.01; ***p < 0.001.

excitatory and inhibitory terminals. This results in an enhanced effect of baclofen on the excitatory pathway in the LSO as compared with the inhibitory pathway.

DISCUSSION

In this study we demonstrate that GABA acts as a retrograde transmitter in the LSO, an auditory brainstem nucleus involved in sound localization, by differentially activating presynaptic GABA$_B$ receptors on the excitatory and inhibitory inputs. We also reveal that GABA$_B$ receptor activity in the LSO fine-tunes the sound localization sensitivity of these neurons. This suggests that adjusting the balance of excitation and inhibition, by means of retrograde release of GABA, might function as an effective control mechanism for the adaptation of auditory brainstem neurons to sound localization sensitivity in the prevailing sound environment.

Retrograde signaling through "classical" neurotransmitters has been shown to contribute to short-term modifications of synaptic efficacy (reviewed by Ludwig and Pittman, 2003; Zilberter et al., 2005). For instance, studies of the neocortex layer 2/3 (Zilberter et al., 1999) and the olfactory bulb (Aroniadou-Anderjaska et al., 2000; Isaacson, 2001; Isaacson and Vitten, 2003; Murphy et al., 2005) have reported that GABA can be released through exocytosis from dendrites. Our results strongly suggest that GABA is released from the dendrites of LSO neurons. This is supported by the fact that many LSO principal cells synthesize GABA (Roberts and Ribak, 1987; Helfert et al., 1989; Gonzalez-Hernandez et al., 1996) and display labeling for VGAT

release machinery, we examined the effects of baclofen on miniature (m)EPSCs/IPSCs (in the presence of 1 μM TTX) and spontaneous (s)EPSCs/IPSCs (in the absence of TTX). Baclofen (10 μM) strongly reduced both the frequency of mEPSCs and sEPSCs (Figures 6A and 6B). In marked contrast, no effect of baclofen was observed on the frequency of mIPSCs (Figure 6A). However, the frequency of the sIPSCs was reduced in the presence of baclofen, in a similar fashion to the sEPSCs (Figure 6B). These results suggest that GABA$_B$ receptor-mediated inhibition of IPSCs is, in contrast to that of the EPSCs, due to inhibition of voltage-dependent Ca^{2+} increases in the presynaptic terminals. To confirm this, we recorded sEPSCs and sIPSCs in the presence of Cd^{2+} (100 μM), a nonspecific Ca^{2+} channel blocker. Cd^{2+} completely blocked the decrease in sIPSC frequency, whereas it caused a less severe decrease in frequency of the baclofen-induced sEPSCs (Figure 6C). It is unlikely that these effects are due to some form of postsynaptic action of baclofen, because the agonist had no effect on the amplitude of the three types of excitatory and inhibitory synaptic events (Figure S4). Taken together, our data support the concept of a mechanism involving differential GABA$_B$ receptor actions on transmitter release from
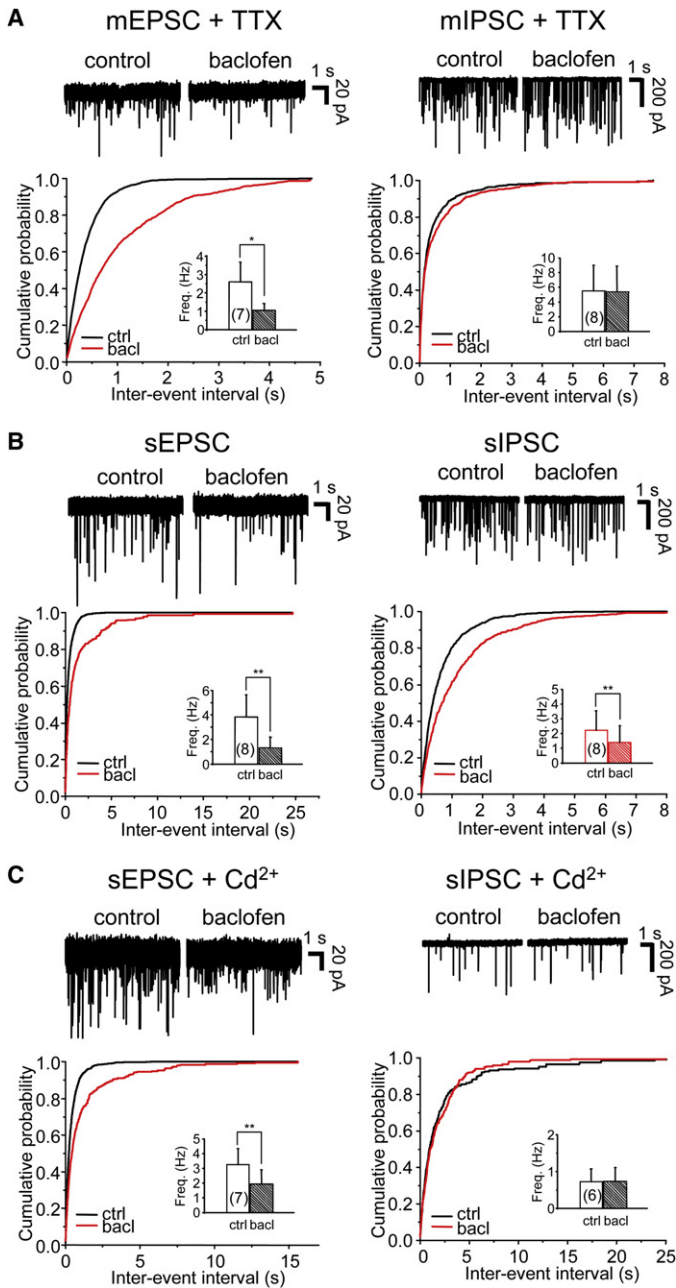
Figure 6. GABA_B Receptor Activation Reduces the Frequency of mEPSCs, but Not mIPSCs

Individual experiments illustrating spontaneous and miniature EPSCs, isolated with strychnine (0.5 μM), and of spontaneous and miniature IPSCs, isolated with DNQX (10 μM), from LSO neurons before and after application of baclofen (10 μM). The sodium channel blocker TTX (1 μM) and the Ca^{2+} channel blocker Cd^{2+} (100 μM) were used to investigate the contribution of (A) action-potential-independent transmitter release, (B) action-potential-dependent and -independent transmitter release, and (C) Ca^{2+}-dependent transmitter release. Graphs illustrate the cumulative distribution of interevent intervals of postsynaptic currents under the control condition (black lines) and during baclofen application (red lines). The insets show the mean postsynaptic current frequency recorded from LSO cells in the control condition and during baclofen application. *p < 0.05; **p < 0.01.

Future studies should dissect the contribution of these components to the Ca^{2+}-dependent release of GABA in the LSO. It is also interesting to note that LSO principal neurons, which most likely provide a glutamatergic or glycinergic input to their target nuclei (Glendenning et al., 1992), use GABA as a retrograde transmitter released from their dendrites. A mixed glutamatergic-GABAergic phenotype has indeed been described in granule cells of the hippocampal dentate gyrus (Gutierrez, 2003).

It cannot be ruled out that acoustic stimulation might trigger other sources of GABA release in the LSO; for instance, release from the periolivary brainstem nuclei or descending projections (Coomes Peterson and Schofield, 2007; Thompson and Schofield, 2000). Indeed, GABAergic terminals of unknown origin have been documented in the LSO (Helfert et al., 1992; Korada and Schwartz, 1999). However, when we stimulated regions adjacent to the LSO, a technique that in most cases elicits transmitter release of the fibers stimulated, we never observed any form of GABA-mediated response. Also, bath application of NO711 (20–100 μM), a GABA-uptake blocker of GAT-1, the predominant isoform in the superior olivary complex (Durkin et al., 1995), affected neither evoked EPSCs nor evoked IPSCs (data not shown). In order to ultimately resolve the issue of the putative origins of GABA release under in vivo conditions, selective intracellular stimulation of LSO neurons in combination with pharmacological manipulation of GABA_B receptors had to be employed in the intact animal.

Clearly GABA, released from the LSO neurons, affects the excitatory input more strongly than it affects the inhibitory input. One underlying mechanism seems to be related to differences in GABA_B receptor control of transmitter release at the two types of terminals. Previous studies have shown that presynaptically located GABA_B receptors modulate transmitter release by either inhibiting voltage-gated Ca^{2+} channels (Scholz and Miller, 1991; Takahashi et al., 1998; Isaacson, 1998) or directly interacting with the synaptic release machinery (Scanziani et al., 1992; Dittman and Regehr, 1996; Sakaba and Neher, 2003). Because both types of mechanisms seem to act in tandem at the excitatory terminals in the LSO, this is likely to make them more susceptible to GABA_B receptor-mediated inhibition of transmitter release. It is

(Chaudhry et al., 1998; present study). Furthermore, in this study, the depolarization-induced GABA release from the LSO neurons was completely prevented by intracellular Ca^{2+} buffering and BoNT D. This is consistent with a release mechanism dependent on a rise in the intracellular Ca^{2+} concentrations, such as exocytosis (reviewed by Sudhof, 2004). In the present experiments, elevation of the dendritic Ca^{2+} concentration may have arisen due to activation of voltage-gated Ca^{2+} channels in response to backpropagating action potentials (Spruston et al., 1995; Kaiser et al., 2001). Alternatively, direct Ca^{2+} influx into the dendrites of LSO neurons through Ca^{2+}-permeable receptors could provide an action-potential-independent rise in Ca^{2+} concentration (Caicedo and Eybalin, 1999; Wu and Fu, 1998; Schmid et al., 2001).

also possible that the large diversity among presynaptic Ca^{2+} channels, which remains to be classified in the LSO, may contribute further to the heterogeneous actions of presynaptic $GABA_B$ receptors on the excitatory and inhibitory release pathways (Wu and Saggau, 1997; Lei and McBain, 2003). Another factor that could explain the differential effects of GABA on excitation and inhibition is the spatial distribution of the excitatory and inhibitory inputs on the neurons. Excitatory inputs to LSO neurons terminate predominantly on the dendrites, whereas inhibitory inputs terminate predominantly on the soma (Cant, 1984; Helfert et al., 1992). These anatomical differences imply that dendritic GABA release affects the excitatory inputs more than the inhibitory ones.

In many sensory systems chronic changes in overall activity levels (over a period of days) drive compensatory changes in excitatory and inhibitory synaptic strength, which keep neuronal properties in a working range and promote stability of firing (Kotak et al., 2005). This type of homeostatic plasticity, which is also referred to as "synaptic scaling," is distinct from input-specific synaptic plasticity (reviewed by Turrigiano and Nelson, 2004; Wierenga et al., 2005). The short-term presynaptic gain control mechanism observed in the present study is probably not a form of "homeostatic synaptic scaling," but rather represents a relatively fast fine-tuning of the synaptic dynamics, which in turn will regulate sensory information processing carried out by these neurons.

So, when and how does retrograde GABA release modulate sound localization behavior? At this time, we can only speculate as to which natural situations this mechanism may be useful in. We propose that auditory spatial discrimination improves during retrograde GABA signaling in the LSO as follows: a sound coming from the left is louder at the left ear than at the right ear, which results in neurons in the left LSO firing action potentials (Figure 7A). As a result, the action-potential-induced GABA release from the dendrites depresses the excitatory inputs more than the inhibitory inputs (Figure 7B), causing a shift in the dynamic part of the response toward the direction of the current sound source and narrowing the binaural response area of the neuron (Figure 7C). Since the discharge rates change maximally at the dynamic part of the response in reaction to small changes in sound location, the ILD sensitivity has now adapted to more lateral positions and should improve localization in the corresponding azimuthal area (i.e., subsequent sounds from a similar spatial location might be localized with an enhanced precision). This type of auditory spatial adaptation has indeed been observed in humans, where a preceding sound selectively improves the ability to spatially segregate subsequent sounds from the same direction (Getzmann, 2004). In addition to this change in coding range, activation of presynaptic $GABA_B$ receptor also serves as an adaptive gain control of the ILD function, which is crucial for the accurate encoding of variable input signals such as overall sound intensity (Brenner et al., 2000; Dean et al., 2005). Although neuronal gain control has usually been associated with a shunting of postsynaptic inhibition (Mitchell and Silver, 2003), there is also evidence that activation of presynaptic metabotropic receptors, such as presynaptic metabotropic glutamate receptors, can impose a gain change on the mossy fiber granule cell synapse in the cerebellum in the subsecond timescale (Mitchell and Silver, 2000).
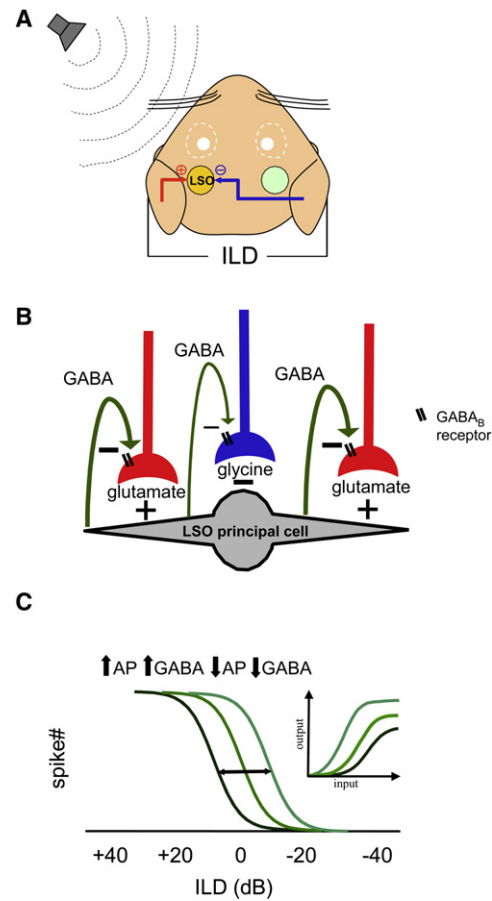
Figure 7. Conceptual Model of Retrograde GABA Signaling in the LSO

(A) Schematic representation of the circuitry encoding ILDs in the gerbil. In this figure, neurons in the left LSO fire action potentials because the sound is louder at the left ear than at the right ear (positive ILDs).

(B) Postsynaptic activity in LSO neurons causes dendritic release of GABA, which activates presynaptic $GABA_B$ receptors on the synaptic terminals. The excitatory input from the ipsilateral ear is more affected than the inhibitory input from the contralateral ear, due to differential regulation of transmitter release by the $GABA_B$ receptors on the respective terminals.

(C) A hypothetical ILD function illustrating how ILD sensitivity is adjusted during more (dotted line) or less (dashed line) action-potential-related (AP) GABA release from an LSO neuron. Note that further GABA release shifts the dynamic range of the response toward the left ear (i.e., ILD sensitivity increases at the side where the sound comes from) and decreases the gain of the input-output function (inset).

Recent experiments from our group show that the response rate of an LSO neuron to a specific ILD is strongly dependent on the ILD of the preceding sound (Park et al., 2008). A similar context-dependent adaptive mechanism has been documented in other sensory systems of the brain where $GABA_B$ receptors sharpen receptive fields (Binns and Salt, 1997; Vucinic et al., 2006). Moreover, as GABA is retrogradely released upon spiking activity of a neuron, the adjustment of the balance of excitation and inhibition should depend on the neuron's previous firing rate. Larger discharge rates ought to weaken excitatory inputs more than inhibitory inputs and thereby also provide an effective

mechanism for monaural self-adaptation. Indeed, a recent study in the inferior colliculus demonstrated that auditory neurons have the capacity to adapt within a few seconds to the most commonly occurring sound levels by adjusting the threshold and the slope of their output function to the statistical distribution of the presented stimuli (Dean et al., 2005). This sensory adaptive phenomenon could be an explanation for the self-adaptive retrograde action of GABA described in the present study. It is also interesting to note that GABA appears to have a similar self-regulatory role in the avian auditory system, in which neurons of the superior olivary nucleus, activated by ipsilateral sound stimulation, send GABAergic backprojections, which serve as a feedback inhibitory control, to several auditory brainstem nuclei (Yang et al., 1999).

A feedback control of synaptic inputs via dendritic release of a neurotransmitter may well be a general mechanism allowing auditory neurons to adapt and extend their range of coding in order to match the sensory environment and accurately represent auditory space.

EXPERIMENTAL PROCEDURES

All experiments were performed in accordance with the rules laid down by the EC Council Directive (86/89/ECC) and German animal welfare legislation.

Single-Unit Recordings and Drug Iontophoresis In Vivo

Gerbils (*Meriones unguiculatus*) were anesthetized with a mixture of Ketamine (10 mg/100 g) and Rompun (2%) throughout the experiment. Animals were placed on a heated cushion in a sound-attenuated chamber and electrodes were inserted stereotaxically through the foramen magnum. Recording electrodes were glass pipettes filled with 2 M sodium acetate (impedance 10–30 MΩ). Action potentials were recorded using conventional methods. Only action potentials from single neurons with a signal-to-noise ratio >5 were recorded. Each recording electrode was attached to a five-barrel glass pipette used for iontophoretic application of drugs, which included the GABA$_B$ agonist baclofen (50 mM; pH 3.5) and two GABA$_B$ antagonists, CGP35348 (100 mM; pH 3.5–4) and CGP55845 (5 mM; pH 3.5). One of the barrels was filled with 4% Horse-Radish-Peroxidase (HRP, Sigma) solution, which was used to mark recording locations for histological reconstructions. Another one of the barrels was filled with sodium acetate (1 M) and served as a balancing channel. Stimuli were delivered using Tucker Davis Technologies (TDT) System II and two Beyer dynamics speakers (model DT 990), fitted to the ears via probe tubes (2 mm inner diameter). The stimulus delivering system and the speakers were calibrated using a 0.25 in microphone (Reinstorp VtS, Germany), a measuring amplifier (MV 302, Microtech, Gefell, Germany), and a waveform analyzer (Stanford Research Systems, model SR770 FFT network analyzer). After electrophysiological isolation of a single neuron, a frequency-tuning curve was measured and the best frequency and threshold were determined. ILD functions were generated by simultaneously presenting 100 ms tones at the neuron's best response frequency. The intensity at the ipsilateral (excitatory) ear was set 20 dB above hearing threshold, whereas the intensity at the contralateral (inhibitory) ear was varied by ± 20–40 dB in a pseudorandom order. Stimuli were delivered at a rate of 4/s with 10 or 20 repetitions at each ILD. The population of neurons used for the two pharmacological manipulations did not differ in their best frequency and 50% ILD. Data were analyzed offline using individual spike times and peristimulus time histograms. Sigmoid curves were fitted to the recorded ILD functions using Matlab (The MathWork Inc., Natick, USA) to determine 50% points and gain of the functions. Only curve fits with $R^2 \geq 0.9$ were included in the data set. For 50% points calculations, the reversal point ILDs of the normalized fitted curves were determined. To assess the gain of the ILD functions, the points of 80% and 20% of maximum response rate of the unnormalized fitted functions were determined, and the slope between the two points was calculated by linear regression.

Whole-Cell Patch-Clamp Recordings In Vitro

Transverse brainstem slices (200 μm) in the area of the superior olivary complex were prepared from gerbils aged P15–21 (3–8 days after hearing onset) as previously described (Magnusson et al., 2005). Slices were transferred to a recording chamber perfused (3–5 ml/min) with oxygenated artificial cerebrospinal fluid (aCSF) at 32°C ± 2°C. Current- and voltage-clamp recordings were made from LSO principal cells using a Multiclamp 700A amplifier (Axon Instruments, Foster City, CA) with standard electrode solutions as described under supplementary materials. During voltage-clamp recordings, the series resistance was lower than 10 MΩ, compensated by 70%–80%, and not allowed to change more than 20%. The principal cells were visually identified by their large fusiform somata with dendrites extending bipolarly. Upon injection of hyperpolarizing and depolarizing currents, these neurons exhibited an onset spike pattern, the typical large voltage-gated conductances in the depolarizing and hyperpolarizing range, and very low input resistance (Figure S2A). Neuron size was estimated from the capacitance compensation measurement under voltage-clamp conditions on the amplifier. Only large neurons with a capacitance larger than 20 pF were included in the analysis. In the gerbil LSO, the large principal cells constitute >75% of the neurons (Helfert and Schwartz, 1987). This makes them a very likely target for in vivo recordings. Also, LSO neurons with very similar intrinsic properties to the ones recorded in the present study have previously been identified as putative principal cells, based on their morphological features and their firing properties in vitro (Adam et al. 1999) and in vivo (Finlayson and Caspary, 1989).

Evoked synaptic responses (interstimulus interval 20–30 ms) were elicited with a glass microelectrode filled with 2 M NaCl, which was positioned in either the fibers coming from the ipsilateral cochlear nucleus or the trapezoid fiber tracts. Isolation of glycinergic or glutamatergic postsynaptic responses was accomplished by addition of 0.5 μM strychnine or 10 μM DNQX, respectively, to the aCSF. During some voltage-clamp recordings, the Ih-blocker ZD7288 (10 μM) was utilized. Experimental protocols and data analysis are described in detail in the Supplementary Material and Methods.

The signals were filtered with a low-pass 4-pole Bessel filter at 10 kHz, sampled at 20–50 kHz and digitized using a Digidata 1322A interface (Axon Instruments, Foster City, CA). Stimulus generation, data acquisition, and offline analysis of data were performed using pClamp Software (Version 9.0 or 10.0; Axon Instruments, Foster City, CA). Results are expressed as mean ± standard deviations in the text and as mean ± 95% confidence intervals in the figures unless otherwise stated. The level of significance was determined by Student's paired or unpaired t test (p < 0.05 was considered statistically significant).

Immunohistochemistry

Gerbils were deeply anesthetized with isofluorane and then perfused transcardially with 0.9% Ringer followed by 4% PFA (n = 4). Brains were removed and postfixed for 6 hr. Tissue was then sectioned at 40 μm with a vibratome. Standard triple immunofluorescent labeling against VGAT (1:400; Chemicon International Inc.), MAP2 (1:250; Labvision Corp.), and Nissl (1:100; Molecular Probes, Germany) was performed (Supplementary Material and Methods). Confocal optical sections were acquired with a Leica TCS SP confocal laser-scanning microscope (Leica Microsystems, Mannheim) equipped with Plan Apo 100 × /1.4 NA oil immersion objective. Fluorochromes were visualized using an argon laser with excitation wavelengths of 488 nm (emission 510–540 nm) for Alexa 488, a DPSS laser with a laser line of 561 nm (emission 565–600 nm) for Cy3, and a helium-neon laser with an excitation wavelength of 633 nm (emission 640−760 nm) for Nissl Deep Red. For each optical section the images were collected sequentially for three fluorochromes. Stacks of eight-bit grayscale images were obtained with axial distances of 300 or 100 nm between optical sections and pixel sizes of 195 to 24 nm depending on the selected zoom factor. After stack acquisition, Z chromatic shift between color channels was corrected. RGB stacks, montages of RGB optical sections, and maximum-intensity projections were created using ImageJ 1.37k plugins. Prior to 3D image reconstructions (generated with Amira 3.1, TGS), 3D data stacks of light optical sections were deconvolved with the Huygens (SVI) maximum-likelihood-estimation algorithm (quality factor 0.1; 20Y40 iterations; signal-to-noise ratio was set to 30) using measured point-spread functions. Surface rendering was applied for the MAP2 staining to highlight the borders of the dendrites.

For the GABA$_B$ immunostaining, sections were prepared as described above (n = 5). Standard immunostaining was performed against the GABA$_B$-R1 subunit of the GABA$_B$ receptor (anti-GABA$_B$-R1, 1:2000, Chemicon International Inc., USA) and subsequently visualized with a DAB protocol (Supplementary Material and Methods).

SUPPLEMENTAL DATA

The Supplemental Data for this article can be found online at http://www.neuron.org/cgi/content/full/59/1/125/DC1/.

REFERENCES

Adam, T.J., Schwarz, D.W., and Finlayson, P.G. (1999). Firing properties of chopper and delay neurons in the lateral superior olive of the rat. Exp. Brain Res. *124*, 489–502.

Aroniadou-Anderjaska, V., Zhou, F.M., Priest, C.A., Ennis, M., and Shipley, M.T. (2000). Tonic and synaptically evoked presynaptic inhibition of sensory input to the rat olfactory bulb via GABA(B) heteroreceptors. J. Neurophysiol. *84*, 1194–1203.

Brenner, N., Bialek, W., and de Ruyter van Stevenick, R. (2000). Adaptive rescaling maximizes information transmission. Neuron *26*, 695–702.

Binns, K.E., and Salt, T.E. (1997). Different roles for GABAA and GABAB receptors in visual processing in the rat superior colliculus. J. Physiol. *504*, 629–639.

Boudreau, J.C., and Tsuchitani, C. (1968). Binaural interaction in the cat superior olive S segment. J. Neurophysiol. *31*, 442–454.

Caicedo, A., and Eybalin, M. (1999). Glutamate receptor phenotypes in the auditory brainstem and mid-brain of the developing rat. Eur. J. Neurosci. *11*, 51–74.

Cant, N.B. (1984). The fine structure of the lateral superior olivary nucleus of the cat. J. Comp. Neurol. *227*, 63–77.

Chang, E.H., Kotak, V.C., and Sanes, D.H. (2003). Long-term depression of synaptic inhibition is expressed postsynaptically in the developing auditory system. J. Neurophysiol. *90*, 1479–1488.

Chaudhry, F.A., Reimer, R.J., Bellocchio, E.E., Danbolt, N.C., Osen, K.K., Edwards, R.H., and Storm-Mathisen, J. (1998). The vesicular GABA transporter, VGAT, localizes to synaptic vesicles in sets of glycinergic as well as GABAergic neurons. J. Neurosci. *18*, 9733–9750.

Coomes Peterson, D., and Schofield, B.R. (2007). Projections from auditory cortex contact ascending pathways that originate in the superior olive and inferior colliculus. Hear. Res. *232*, 67–77.

Dean, I., Harper, N.S., and McAlpine, D. (2005). Neural population coding of sound level adapts to stimulus statistics. Nat. Neurosci. *8*, 1684–1689.

Dittman, J.S., and Regehr, W.G. (1996). Contributions of calcium-dependent and calcium-independent mechanisms to presynaptic inhibition at a cerebellar synapse. J. Neurosci. *16*, 1623–1633.

Durkin, M.M., Smith, K.E., Borden, L.A., Weinshank, R.L., Branchek, T.A., and Gustafson, E.L. (1995). Localization of messenger RNAs encoding three GABA transporters in rat brain: an in situ hybridization study. Brain Res. Mol. Brain Res. *33*, 7–21.

Dutia, M.B., Johnston, A.R., and McQueen, D.S. (1992). Tonic activity of rat medial vestibular nucleus neurones in vitro and its inhibition by GABA. Exp. Brain Res. *88*, 466–472.

Finlayson, P.G., and Caspary, D.M. (1989). Synaptic potentials of chinchilla lateral superior olivary neurons. Hear. Res. *38*, 221–228.

Getzmann, S. (2004). Spatial discrimination of sound sources in the horizontal plane following an adapter sound. Hear. Res. *191*, 14–20.

Glendenning, K.K., Baker, B.N., Hutson, K.A., and Masterton, R.B. (1992). Acoustic chiasm V: inhibition and excitation in the ipsilateral and contralateral projections of LSO. J. Comp. Neurol. *319*, 100–122.

Gonzalez-Hernandez, T., Mantolan-Sarmiento, B., Gonzalez-Gonzalez, B., and Perez-Gonzalez, H. (1996). Sources of GABAergic input to the inferior colliculus of the rat. J. Comp. Neurol. *372*, 309–326.

Gutierrez, R. (2003). The GABAergic phenotype of the "glutamatergic" granule cells of the dentate gyrus. Prog. Neurobiol. *71*, 337–358.

Helfert, R.H., and Schwartz, I.R. (1987). Morphological features of five neuronal classes in the gerbil lateral superior olive. Am. J. Anat. *179*, 55–69.

Helfert, R.H., Bonneau, J.M., Wenthold, R.J., and Altschuler, R.A. (1989). GABA and glycine immunoreactivity in the guinea pig superior olivary complex. Brain Res. *501*, 269–286.

Helfert, R.H., Juiz, J.M., Bledsoe, S.C., Jr., Bonneau, J.M., Wenthold, R.J., and Altschuler, R.A. (1992). Patterns of glutamate, glycine, and GABA immunolabeling in four synaptic terminal classes in the lateral superior olive of the guinea pig. J. Comp. Neurol. *323*, 305–325.

Higley, M.J., and Contreras, D. (2006). Balanced excitation and inhibition determine spike timing during frequency adaptation. J. Neurosci. *26*, 448–457.

Holstein, G.R., Martinelli, G.P., and Cohen, B. (1992). L-baclofen-sensitive GABAB binding sites in the medial vestibular nucleus localized by immunocytochemistry. Brain Res. *581*, 175–180.

Isaacson, J.S. (1998). GABAB receptor-mediated modulation of presynaptic currents and excitatory transmission at a fast central synapse. J. Neurophysiol. *80*, 1571–1576.

Isaacson, J.S. (2001). Mechanisms governing dendritic gamma-aminobutyric acid (GABA) release in the rat olfactory bulb. Proc. Natl. Acad. Sci. USA *98*, 337–342.

Isaacson, J.S., and Vitten, H. (2003). GABAB receptors inhibit dendrodendritic transmission in the rat olfactory bulb. J. Neurosci. *23*, 2032–2039.

Kaiser, K.M.M., Zilberter, Y., and Sakmann, B. (2001). Back-propagating action potentials mediate calcium signalling in dendrites of bitufted interneurons in layer 2/3 of rat somatosensory cortex. J. Physiol. *535*, 17–31.

Korada, S., and Schwartz, I.R. (1999). Development of GABA, glycine, and their receptors in the auditory brainstem of gerbil: a light and electron microscopic study. J. Comp. Neurol. *409*, 664–681.

Kotak, V.C., DiMattina, C., and Sanes, D.H. (2001). GABA(B) and Trk receptor signaling mediates long-lasting inhibitory synaptic depression. J. Neurophysiol. *86*, 536–540.

Kotak, V.C., Fujisawa, S., Lee, F.A., Karthikeyan, O., Aoki, C., and Sanes, D.H. (2005). Hearing loss raises excitability in the auditory cortex. J. Neurosci. *25*, 3908–3918.

Lei, S., and McBain, C.J. (2003). GABAB receptor modulation of excitatory and inhibitory synaptic transmission onto rat CA3 hippocampal interneurons. J. Physiol. *546*, 439–453.

Ludwig, M., and Pittman, Q.J. (2003). Talking back: dendritic neurotransmitter release. Trends Neurosci. *26*, 255–261.

Magnusson, A.K., Kapfer, C., Grothe, B., and Koch, U. (2005). Maturation of glycinergic inhibition in the gerbil medial superior olive after hearing onset. J. Physiol. *568*, 497–512.

Marino, J., Schummers, J., Lyon, D.C., Schwabe, L., Beck, O., Wiesing, P., Obermayer, K., and Sur, M. (2005). Invariant computations in local cortical networks with balanced excitation and inhibition. Nat. Neurosci. *8*, 194–201.

Miller, R.J. (1998). Presynaptic receptors. Annu. Rev. Pharmacol. Toxicol. *38*, 201–227.

Mitchell, S.J., and Silver, R.A. (2000). Glutamate spillover suppresses inhibition by activating presynaptic mGluRs. Nature *404*, 498–502.

Mitchell, S.J., and Silver, R.A. (2003). Shunting inhibition modulates neuronal gain during synaptic excitation. Neuron *38*, 433–445.

Moore, M.J., and Caspary, D.M. (1983). Strychnine blocks binaural inhibition in lateral superior olivary neurons. J. Neurosci. *3*, 237–242.

Murphy, G.J., Darcy, D.P., and Isaacson, J.S. (2005). Intraglomerular inhibition: signaling mechanisms of an olfactory microcircuit. Nat. Neurosci. *8*, 354–364.

Nicoll, R.A. (2004). My close encounter with GABAB receptors. Biochem. Pharmacol. *68*, 1667–1674.

Park, T.J., Grothe, B., Pollak, G.D., Schuller, G., and Koch, U. (1996). Neural delays shape selectivity to interaural intensity differences in the lateral superior olive. J. Neurosci. *16*, 6554–6566.

Park, T.J., Brand, A., Koch, U., and Grothe, B. (2008). Dynamic changes in level influence spatial coding in the lateral superior olive. Hear. Res. *238*, 58–67.

Roberts, R.C., and Ribak, C.E. (1987). GABAergic neurons and axon terminals in the brainstem auditory nuclei of the gerbil. J. Comp. Neurol. *258*, 267–280.

Sakaba, T., and Neher, E. (2003). Direct modulation of synaptic vesicle priming by GABAB receptor activation at a glutamatergic synapse. Nature *424*, 775–778.

Sanes, D.H., Geary, W.A., Wooten, G.F., and Rubel, E.W. (1987). Quantitative distribution of the glycine receptor in the auditory brain stem of the gerbil. J. Neurosci. *7*, 3793–3802.

Scanziani, M., Capogna, M., Gahwiler, B.H., and Thompson, S.M. (1992). Presynaptic inhibition of miniature excitatory synaptic currents by baclofen and adenosine in the hippocampus. Neuron *9*, 919–927.

Schmid, S., Guthmann, A., Ruppersberg, J.P., and Herbert, H. (2001). Expression of AMPA receptor subunit flip/flop splice variants in the rat auditory brainstem and inferior colliculus. J. Comp. Neurol. *430*, 160–171.

Schoch, S., Deak, F., Konigstorfer, A., Mozhayeva, M., Sara, Y., Sudhof, T.C., and Kavalali, E.T. (2001). SNARE function analyzed in synaptobrevin/VAMP knockout mice. Science *294*, 1117–1122.

Scholz, K.P., and Miller, R.J. (1991). GABAB receptor-mediated inhibition of Ca2+ currents and synaptic transmission in cultured rat hippocampal neurones. J. Physiol. *444*, 669–686.

Spruston, N., Schiller, Y., Stuart, G., and Sakmann, B. (1995). Activity-dependent action potential invasion and calcium influx into hippocampal CA1 dendrites. Science *268*, 297–300.

Sudhof, T.C. (2004). The synaptic vesicle cycle. Annu. Rev. Neurosci. *27*, 509–547.

Takahashi, T., Kajikawa, Y., and Tsujimoto, T. (1998). G-Protein-Coupled Modulation of Presynaptic Calcium Currents and Transmitter Release by a GABAB Receptor. J. Neurosci. *18*, 3138–3146.

Thompson, A.M., and Schofield, B.R. (2000). Afferent projections of the superior olivary complex. Microsc. Res. Tech. *51*, 330–354.

Turrigiano, G.G., and Nelson, S.B. (2004). Homeostatic plasticity in the developing nervous system. Nat. Rev. Neurosci. *5*, 97–107.

Vucinic, D., Cohen, L.B., and Kosmidis, E.K. (2006). Interglomerular center-surround inhibition shapes odorant-evoked input to the mouse olfactory bulb in vivo. J. Neurophysiol. *95*, 1881–1887.

Wehr, M., and Zador, A.M. (2003). Balanced inhibition underlies tuning and sharpens spike timing in auditory cortex. Nature *426*, 442–446.

Wierenga, C.J., Ibata, K., and Turrigiano, G.G. (2005). Postsynaptic expression of homeostatic plasticity at neocortical synapses. J. Neurosci. *25*, 2895–2905.

Wu, L.G., and Saggau, P. (1997). Presynaptic inhibition of elicited neurotransmitter release. Trends Neurosci. *20*, 204–212.

Wu, S.H., and Fu, X.W. (1998). Glutamate receptors underlying excitatory synaptic transmission in the rat's lateral superior olive studied in vitro. Hear. Res. *122*, 47–59.

Yang, L., Monsivais, P., and Rubel, E.W. (1999). The superior olivary nucleus and its influence on nucleus laminaris: a source of inhibitory feedback for coincidence detection in the avian auditory brainstem. J. Neurosci. *19*, 2313–2325.

Zhang, L.I., Tan, A.Y., Schreiner, C.E., and Merzenich, M.M. (2003). Topography and synaptic shaping of direction selectivity in primary auditory cortex. Nature *424*, 201–205.

Zilberter, Y., Kaiser, K.M.M., and Sakmann, B. (1999). Dendritic GABA release depresses excitatory transmission between layer 2/3 pyramidal and bitufted neurons in rat neocortex. Neuron *24*, 979–988.

Zilberter, Y., Harkany, T., and Holmgren, C.D. (2005). Dendritic release of retrograde messengers controls synaptic transmission in local neocortical networks. Neuroscientist *11*, 334–344.